

$\delta = 0.04$  (s, 36H, SiMe<sub>3</sub>), 6.92–7.11 (m, 24H, Ph), 7.40–7.74 (m, 16H, Ph); <sup>13</sup>C{<sup>1</sup>H} NMR (75.47 MHz, C<sub>6</sub>D<sub>6</sub>, 25 °C, TMS):  $\delta = 3.65$  (SiMe<sub>3</sub>), 130.09, 132.87, 139.25, 140.44 (Ph); <sup>31</sup>P{<sup>1</sup>H} NMR (161.92 MHz, C<sub>6</sub>D<sub>6</sub>, 25 °C, 80 % H<sub>3</sub>PO<sub>4</sub>):  $\delta = 12.34$ .

Received: January 18, 2001

Revised: March 22, 2001 [Z 16444]

## A Synthetic Pore-Mediated Transmembrane Transport of Glutamic Acid\*\*

Jorge Sánchez-Quesada, Hui Sun Kim, and M. Reza Ghadiri\*

Synthetic constructs that are specifically designed to allow transport of hydrophilic substances across cell membranes are important research tools with possible applications in gene and antisense therapy, metabolite regulation, and drug delivery.<sup>[1]</sup> However, surprisingly the design of synthetic transmembrane pores from first principles has remained largely unexplored.<sup>[2, 3]</sup> Here we describe the design and functional characterization of a self-assembling transmembrane peptide nanotube channel that is capable of highly efficient transport of L-glutamic acid.

Appropriately designed cyclic peptides with an even number of hydrophobic  $\alpha$ -amino acids with alternating D and L configurations have been previously shown to self-assemble through directed hydrogen-bonding networks into antiparallel  $\beta$ -sheet tubular structures in lipid bilayers forming active ion channels.<sup>[4]</sup> One attractive feature of the self-assembling peptide nanotube class of transmembrane supramolecular structures is that pore size can be tuned by the choice<sup>[5]</sup> and the number of  $\alpha$ -amino acids employed in the cyclic peptide subunit design. In this context we have shown previously that cyclic octapeptides size-selectively transport small ions,<sup>[4, 6]</sup> whereas decapeptides can also transport small molecules such as glucose.<sup>[3]</sup>


The present system is based on eight- and ten-residue cyclic peptides **1**<sup>[4]</sup> and **2**,<sup>[3]</sup> respectively, which form transmembrane channels (Scheme 1). Inspection of space-filling models derived from X-ray structural analogues of peptide nanotubes suggests that a completely dehydrated glutamate ion in an extended conformation would barely fit inside a channel formed by the cyclic octapeptide **1** (7 Å van der Waals internal diameter) but could be easily accommodated in a transmembrane pore derived from cyclic decapeptide **2** (10 Å van der Waals internal diameter).<sup>[3]</sup> We therefore sought to examine the utility of self-assembling peptide nanotubes for size-selective transmembrane transport of glutamate ions.

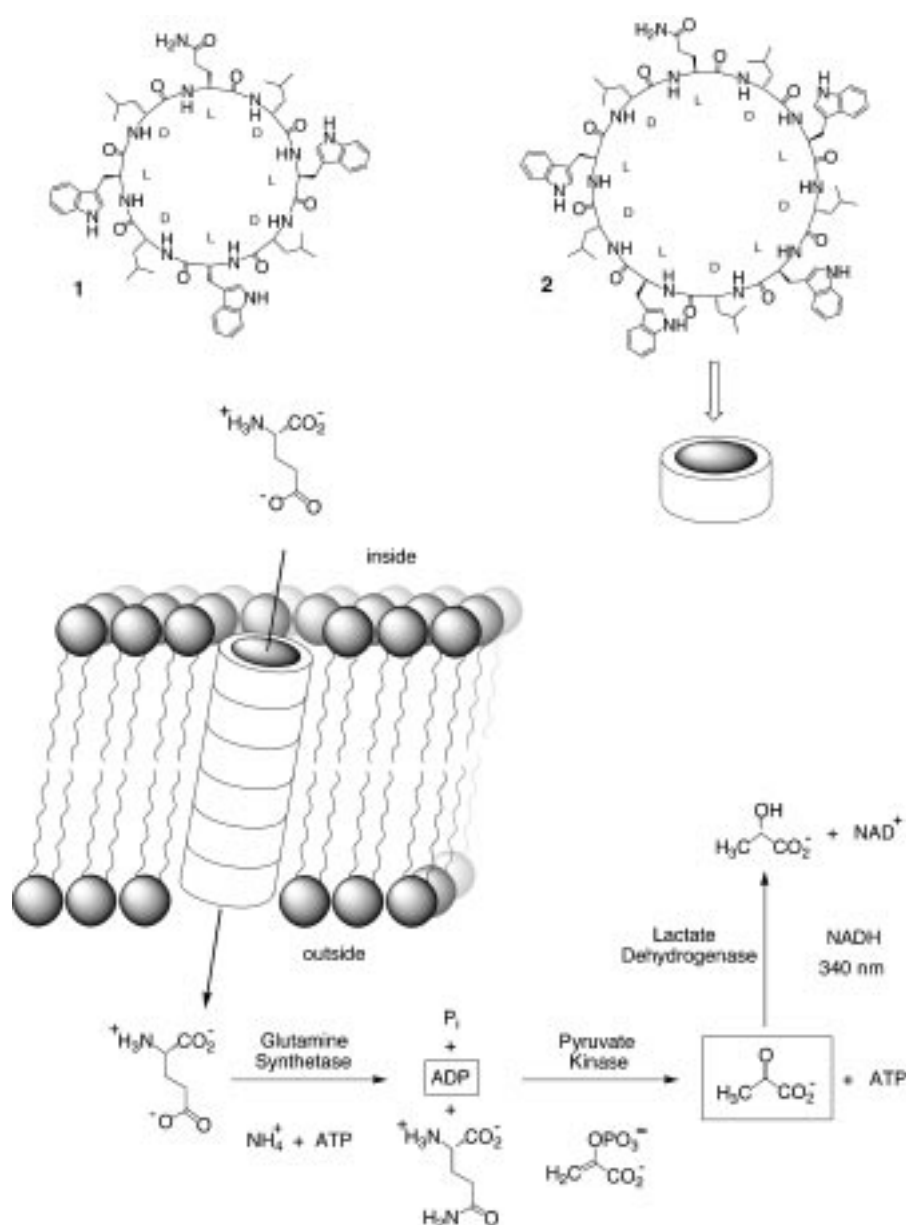
Previous attenuated total reflection/Fourier transform infrared (ATR-FTIR) spectroscopic studies of the peptide **1** in lipid multibilayers indicated that the self-assembled transmembrane channel adopts an orientation of  $7 \pm 1^\circ$  relative to the average plane of membrane.<sup>[7]</sup> In analogous studies for decapeptide **2**, the peptide assembly in the lipid bilayer displayed backbone amide bands indicative of the expected

- [1] a) J. Escudie, H. Ranaivonjatovo, *Adv. Organomet. Chem.* **1999**, *44*, 113; b) M. Driess, H. Grützmacher, *Angew. Chem.* **1996**, *108*, 900; *Angew. Chem. Int. Ed. Engl.* **1996**, *35*, 828.
- [2] H. Leclercq, I. Dubois, *J. Mol. Spectrosc.* **1979**, *76*, 39.
- [3] M. Izuha, S. Yamamoto, D. Saito, *J. Chem. Phys.* **1996**, *105*, 4923.
- [4] W. H. Harper, E. A. Ferrall, R. K. Hilliard, S. M. Stogner, R. S. Grev, D. J. Clouthier, *J. Am. Chem. Soc.* **1997**, *119*, 8361.
- [5] S. M. Stogner, R. S. Grev, *J. Chem. Phys.* **1998**, *108*, 5458.
- [6] C. M. Ong, D. W. Stephan, *J. Am. Chem. Soc.* **1999**, *121*, 2939.
- [7] S. I. Al-Resayes, P. B. Hitchcock, J. F. Nixon, *J. Chem. Soc. Chem. Commun.* **1986**, 1710.
- [8] J. Browning, K. R. Dixon, R. W. Hilts, *Organometallics* **1989**, *8*, 552.
- [9] A. Kasani, R. McDonald, M. Ferguson, R. G. Cavell, *Organometallics* **1999**, *18*, 4241.
- [10] R. P. Kamalesh Babu, R. McDonald, R. G. Cavell, *Chem. Commun.* **2000**, 481.
- [11] A. Kasani, M. Ferguson, R. G. Cavell, *J. Am. Chem. Soc.* **2000**, *122*, 726.
- [12] Crystal data for **2** (C<sub>64</sub>H<sub>81</sub>Ge<sub>2</sub>N<sub>4</sub>O<sub>0.5</sub>P<sub>4</sub>Si<sub>4</sub>):  $M = 1295.75$ , crystal size  $0.60 \times 0.45 \times 0.25$  mm,  $a = 21.030(4)$ ,  $b = 16.453(3)$ ,  $c = 19.919(4)$  Å,  $\alpha = 90^\circ$ ,  $\beta = 91.62(3)^\circ$ ,  $\gamma = 90^\circ$ ,  $V = 6890(2)$  Å<sup>3</sup>,  $\rho_{\text{calcd}} = 1.249$  g cm<sup>-3</sup>,  $\mu = 1.075$  mm<sup>-1</sup>,  $Z = 4$ , monoclinic, space group  $P2_1/c$ ,  $\lambda = 0.71073$  Å,  $T = 293(2)$  K,  $2\theta_{\text{max}} = 48^\circ$ , 11 779 measured reflections, 10 823 independent and 5511 observed reflections ( $I > 2\sigma(I)$ ), 697 refined parameters,  $R1 = 0.0725$ ,  $wR2 = 0.1843$ , largest diff. peak and hole 0.3833 and  $-0.696$  e Å<sup>-3</sup>. Crystal data for **3** (C<sub>62</sub>H<sub>76</sub>N<sub>4</sub>P<sub>4</sub>Pb<sub>2</sub>Si<sub>4</sub>):  $M = 152.89$ , crystal size  $0.78 \times 0.19 \times 0.17$  mm,  $a = 10.4752(14)$ ,  $b = 44.827(6)$ ,  $c = 14.068(2)$  Å,  $\alpha = 90^\circ$ ,  $\beta = 100.796(3)^\circ$ ,  $\gamma = 90^\circ$ ,  $V = 6489.0(15)$  Å<sup>3</sup>,  $\rho_{\text{calcd}} = 1.564$  g cm<sup>-3</sup>,  $\mu = 5.395$  mm<sup>-1</sup>,  $Z = 4$ , monoclinic, space group  $P2_1/n$ ,  $\lambda = 0.71073$  Å,  $T = 293(2)$  K,  $\phi/\omega$  scans,  $2\theta_{\text{max}} = 56.22^\circ$ , 45 654 measured reflections, 15 684 independent and 8598 observed reflections ( $I > 2\sigma(I)$ ), 686 refined parameters,  $R1 = 0.0468$ ,  $wR2 = 0.0804$ , largest diff. peak and hole 1.356 and  $-1.686$  e Å<sup>-3</sup>. The crystal data were measured on an IP Rigaku diffractometer (for **2**) or a Bruker SMART CCD area detector (for **3**). The structures were solved by direct methods using SHELXS-97 and refined using SHELXL-97. Crystallographic data (excluding structure factors) for the structures reported in this paper have been deposited with the Cambridge Crystallographic Data Centre as supplementary publication no. CCDC-160423 and 160424. Copies of the data can be obtained free of charge on application to CCDC, 12 Union Road, Cambridge CB21EZ, UK (fax: (+44) 1223-336-033; e-mail: deposit@ccdc.cam.ac.uk).
- [13] K. M. Baines, W. G. Stibbs, *Adv. Organomet. Chem.* **1996**, *39*, 275.
- [14] W.-P. Leung, W.-H. Kwok, F. Xue, T. C. W. Mak, *J. Am. Chem. Soc.* **1997**, *119*, 1145.
- [15] W.-P. Leung, H. Cheng, R.-B. Huang, Q.-C. Yang, T. C. W. Mak, *Chem. Commun.* **2000**, 451.
- [16] H. J. Meyer, G. Baum, W. Massa, S. Berger, A. Berndt, *Angew. Chem.* **1987**, *99*, 559; *Angew. Chem. Int. Ed. Engl.* **1987**, *26*, 546.
- [17] W.-P. Leung, W.-H. Kwok, L.-H. Weng, L. T. C. Law, Z.-Y. Zhou, T. C. W. Mak, *J. Chem. Soc. Dalton Trans.* **1997**, 4301.

[\*] Prof. M. R. Ghadiri, Dr. J. Sánchez-Quesada, Dr. H. Sun Kim  
Departments of Chemistry and Molecular Biology, and  
The Skaggs Institute for Chemical Biology  
The Scripps Research Institute  
10550 North Torrey Pines Road, La Jolla, CA 92037 (USA)  
Fax: (+1) 858-784-2798  
E-mail: ghadiri@scripps.edu

[\*\*] This work is supported by a grant from the National Institutes of Health (Grant: GM52190).

 Supporting information for this article is available on the WWW under <http://www.angewandte.com> or from the author.



Scheme 1. Chemical structures of cyclooctapeptide **1** and cyclodecapeptide **2**, and the reaction scheme employed for the analysis of glutamic acid transport. The enzymes and cofactors reside in the extravesicular milieu, and are hydrophilic and too large to penetrate the lipid bilayer. Therefore, only the glutamic acid released upon introduction of the channel-forming peptide, can undergo the enzymatic reaction noted.

hydrogen-bonded antiparallel  $\beta$ -sheet tubular structure: amide I bands at 1635 (perpendicular component, strong) and 1691  $\text{cm}^{-1}$  (parallel component, weak), an amide II band at 1539  $\text{cm}^{-1}$ , and an amide A (N–H stretch) band at  $\sim 3285 \text{ cm}^{-1}$  (Figure 1). The longitudinal axis of the peptide channel assembly was determined to be oriented approximately perpendicular to the membrane plane, at an angle of  $3 \pm 2^\circ$  from the lipid hydrocarbon chain tilt.<sup>[8]</sup> These results are consistent with the membrane-spanning orientation of the tubular assemblies required for an intrapore-mediated mode of transport.

Channel-mediated glutamic acid transport from the inside of large unilamellar vesicles to the external solvent under isotonic solution conditions was continuously monitored by

an enzymatic assay operating in the extravesicular milieu (Scheme 1). This highly sensitive spectrophotometric assay couples glutamine synthetase activity with the reactions catalyzed by pyruvate kinase and lactate dehydrogenase, by monitoring NADH oxidation at 340 nm. The pyruvate kinase and lactate dehydrogenase were added in appropriate excess of the glutamine synthetase, and glutamine synthetase has a high catalytic efficiency, so the observed rate of NADH oxidation was directly proportional to the vesicular release of glutamic acid.<sup>[9]</sup>

The transport activity mediated by the ten-residue cyclic peptide ensemble **2** showed a saturation-type behavior, due to the limited peptide solubility in the lipid bilayer, and displayed an apparent rate constant of approximately 2.0 mol of glutamic acid per minute per 1.0 M cyclic peptide for vesicles containing 500 mM glutamic acid in the presence of 1.0  $\mu\text{M}$  peptide **2** (Figure 2a).<sup>[10]</sup> Control fluorescence experiments using vesicle-entrapped carboxyfluorescein dye molecules indicated that the release of glutamic acid to the extravesicular milieu is not due to the rupture of the lipid vesicles. Furthermore, neither the octapeptide **1** nor gramicidin<sup>[11]</sup> (which form channels with, respectively,  $\sim 7$  and  $\sim 2.6 \text{ \AA}$  van der Waals internal diameters) showed glutamate transport activity under similar assay conditions (Figure 2b).

We investigated the ion-channel behavior for peptides **1** and **2** by performing single-channel conductance experiments in planar lipid bilayers.<sup>[12]</sup> Conductance  $I$  measured at different

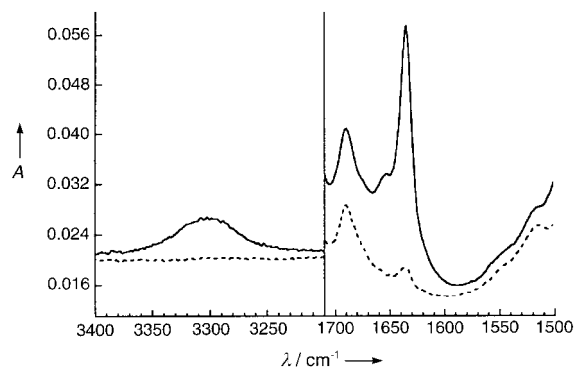


Figure 1. ATR-FTIR spectrum of the amide regions of **2** in a 1,2-myristoyl-*sn*-glycero-3-phosphatidylcholine multibilayer film. The solid and dotted lines indicate absorption of parallel and perpendicular polarized light, respectively.

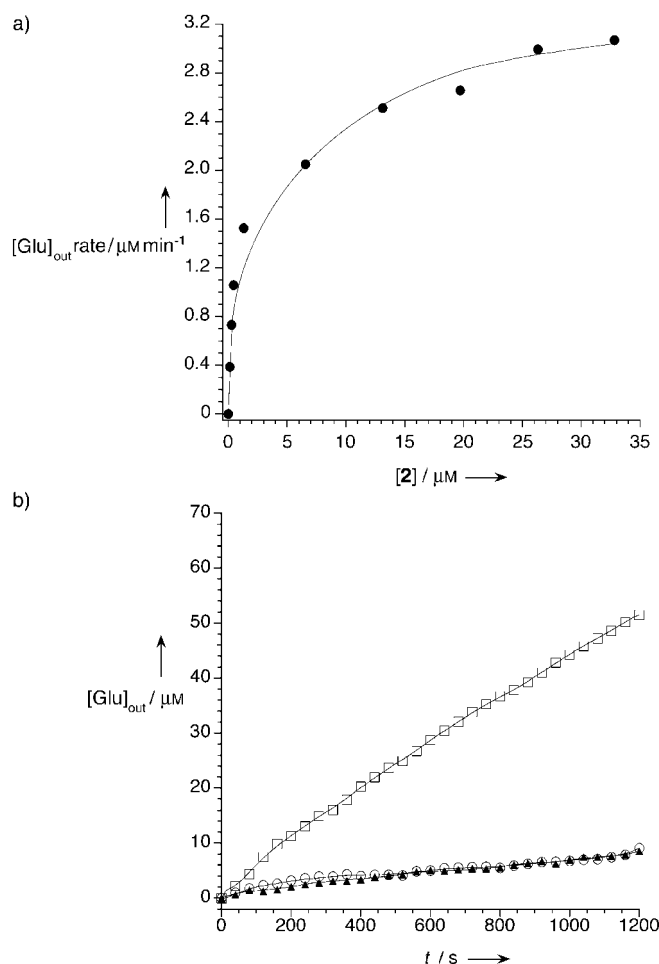


Figure 2. a) The glutamate efflux rate ( $[\text{Glu}]_{\text{out}} \text{ rate}$ ) from vesicles is dependent on the initial concentrations of the cyclic peptide **2**; b) glutamate efflux ( $[\text{Glu}]_{\text{out}}$ ) from vesicles over time, after the addition of 13.1  $\mu\text{M}$  quantities of each the following compounds: gramicidin A ( $\blacktriangle$ ), octapeptide peptide **1** ( $\circ$ ), and decapeptide **2** ( $\square$ ).

NaCl concentrations could be fitted to a Michaelis–Menten saturation model for both cyclopeptides ( $A_{\text{max}} = 11.5 \pm 0.3 \text{ pS}$ ,  $K_M = 8.1 \pm 1.9 \text{ mM}$  for **1**;  $A_{\text{max}} = 13.0 \pm 0.5 \text{ pS}$ ,  $K_M = 28.1 \pm 5.6 \text{ mM}$  for **2**; Figure 3a and b); this indicates that channel occupancy is restricted to a single ion.<sup>[13]</sup> On the other hand, whereas the open probabilities  $P_{\text{open}}$  were similar ( $0.25 \pm 0.05$  and  $0.27 \pm 0.04$  for **1** and **2**, respectively), the mean opening times (Figure 3c and d) were longer for the octapeptide channel ( $\tau = 1340 \pm 50 \text{ ms}$ ) than for the decapeptide channel ( $\tau = 168 \pm 12 \text{ ms}$ ), as expected due to the greater conformational freedom in **2**. Reverse potential determination from experiments employing asymmetric NaCl concentrations revealed total cation selectivity for these cyclic peptide based channels, similar to that observed for gramicidin A under the same conditions (Table 1).

With these data at hand we then turned to study the behavior of these transmembrane channels when the monosodium salt of glutamic acid (NaGlu) was employed as the electrolyte. Although tabulated activity coefficients for NaGlu in bulk solutions are available,<sup>[14]</sup>

Table 1. Reversal potentials for gramicidin A (gram.), and the cyclic peptides **1** and **2** with “asymmetric” NaCl concentrations.

	$c/t^{[a]}$		
	100/300	100/500	100/1000
$E_r \text{ calcd} [\text{mV}]^{[b]}$	−24.9	−36.5	−52.8
$E_r \text{ gram.} [\text{mV}]$	$-27.9 \pm 0.1$	$-40.4 \pm 0.1$	$-55.4 \pm 0.1$
$E_r \text{ 1} [\text{mV}]$	$-28.2 \pm 0.1$	$-41.1 \pm 0.2$	$-55.1 \pm 0.6$
$E_r \text{ 2} [\text{mV}]$	$-26.9 \pm 0.4$	$-40.9 \pm 0.6$	$-54.2 \pm 1.2$

[a]  $c/t$  refers to the ratio of the NaCl concentrations (mM) on the cis (c) and trans (t) sides of the lipid bilayer. [b] The reverse potentials,  $E_r$ , were calculated with the GHK equation.

they are not appropriate in the present studies since the activity coefficients are expected to be altered in buffered solutions and/or by interactions of the electrolyte components with the polar lipid head groups. Therefore, we directly measured the activities of NaGlu by employing gramicidin A as a standard whose transmembrane pore diameter is known to be too small to allow glutamate transport. We measured the biionic potential for gramicidin in planar lipid bilayers separating isotonic NaCl on the cis side and NaGlu on the trans side (Figure 4, Table 2); it was then possible to calculate the activities for the NaGlu solutions with the GHK equation.<sup>[15]</sup> The biionic potential for the octapeptide **1** observed under the same conditions was comparable to that obtained with gramicidin, which indicates no glutamate

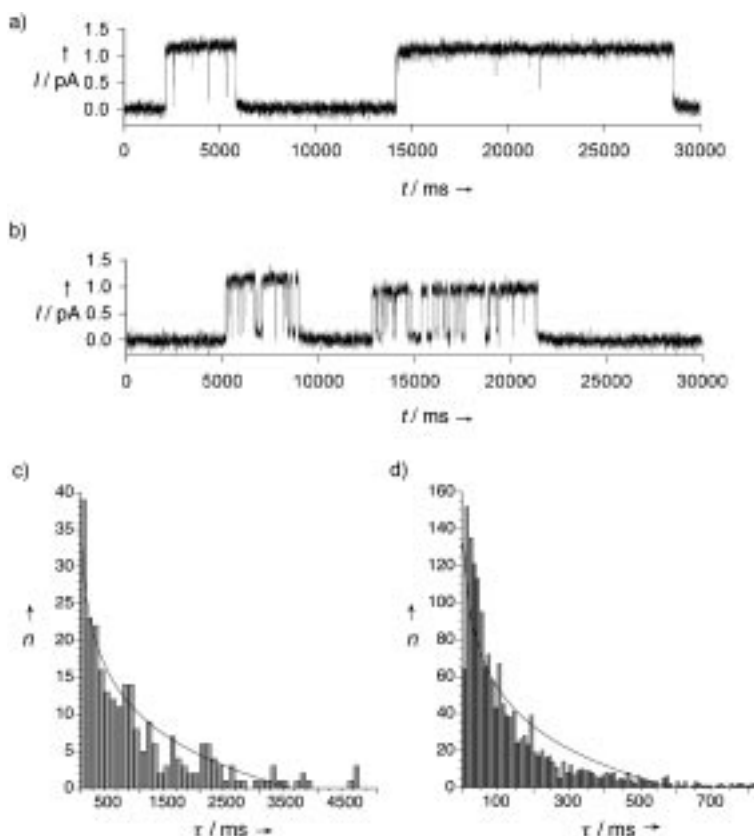


Figure 3. Traces showing 30 seconds of channel activity for a) **1** and b) **2** in 100 mM NaCl at a transmembrane holding potential of +100 mV. Signals were Bessel filtered at 5 kHz and sampled at 100  $\mu\text{s}$ . Dwell time histograms for c) **1** and d) **2** obtained from traces recorded in 100 mM NaCl at a transmembrane potential of +100 mV.  $I$  = current,  $n$  = number of observations,  $\tau$  = dwell time.

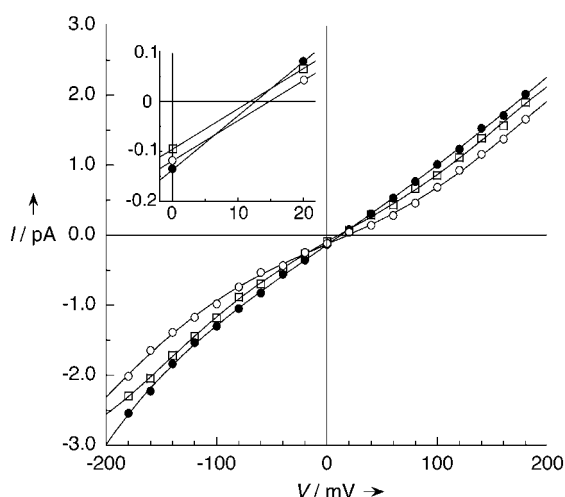


Figure 4. Current/voltage ( $I/V$ ) plot for gramicidin A (●), **1** (□), and **2** (○) in lipid bilayers separating isotonic 300 mM NaCl and NaGlu on the cis and trans sides, respectively.  $I/V$  curves are averaged from 30 individual  $I/V$  experiments. The inset shows the higher reversal potential for peptide **2**.

Table 2. Reverse potentials and permeability ratios for gramicidin A (gram.), and the cyclic peptides **1** and **2** obtained for NaCl and NaGlu solutions on the cis and trans sides of the lipid bilayer, respectively.

	$c/t^{[a]}$		
	100/100	300/300	1000/1000
$E_r$ gram. [mV]	$11.3 \pm 0.7$	$12.6 \pm 0.8$	$13.1 \pm 0.7$
$E_r$ <b>1</b> [mV]	$11.8 \pm 0.6$	$11.8 \pm 1.1$	$12.3 \pm 0.9$
$E_r$ <b>2</b> [mV]	$13.7 \pm 0.6$	$14.8 \pm 0.6$	$15.3 \pm 0.5$
NaGlu activity <sup>[b]</sup>	$0.049 \pm 0.001$	$0.128 \pm 0.004$	$0.201 \pm 0.006$
$P_{Na^+}/P_{Glu^-}^{[c]}$ <b>2</b>	$6.3 \pm 0.7$	$6.5 \pm 1.1$	$6.3 \pm 0.9$

[a]  $c/t$  refers to the ratio of the NaCl and NaGlu concentrations (mM) on the cis (c) and trans (t) sides of the lipid bilayer, respectively. [b] Activities for sodium glutamate (NaGlu) were calculated from the measured biionic potential with gramicidin A and the GHK equation. [c] Permeability ratios for sodium and glutamate ions with decapeptide **2** were calculated with the GHK equation. Activities for sodium glutamate solutions were taken from the experiments where gramicidin A was used as a standard.

transport with pores formed by **1** (Figure 4, Table 2). However, with **2** a higher potential needs to be applied to counteract the chemical gradient (Figure 4, Table 2) and this indicates a substantial transport of the aminoacid ( $P_{Na^+}/P_{Glu^-} = 6.4 \pm 0.9$ ). Considering that  $P_{open}$  is about 0.27 and assuming an average of six cyclic peptides per assembly (28 Å length, enough to span a lipid bilayer), in bilayers separating 0.5 M NaGlu and NaCl at 0 V ( $I = 0.19$  pA), the rate of transport can be evaluated as  $2.7 \times 10^4$  mol of glutamate per second per 1.0 M cyclic peptide.

In conclusion, we have described the first example of highly efficient aminoacid transport by a de novo designed channel system. This study indicates potential utility for this class of biomaterials in biosensor applications as well as in biological settings such as size-selective molecular delivery vehicles.

Received: February 1, 2001 [Z16543]

- [1] For recent reviews on colloid-based drug delivery agents, see: a) N. V. Majeti, M. N. V. Ravi Kumar, *J. Pharm. Sci.* **2000**, *3*, 234–258; b) G. M. Barat, *Pharm. Sci. Technol. Today* **2000**, *3*, 163–171. For dendrimers, see: c) H. Yoo, P. Sazani, R. L. Juliano, *Pharm. Res.* **1999**,

- 16*, 1799–1804; d) M. Liu, K. Kono, J. M. J. Frechet, *J. Controlled Release* **2000**, *65*, 121–131; e) L. G. Schultz, S. C. Zimmerman, *Pharm. News* **1999**, *6*, 25–29. For polymers, see: f) D. C. Bibby, N. M. Davies, I. G. Tucker, *Int. J. Pharm.* **2000**, *197*, 1–11. For liquid crystals as drug delivery agents, see: g) F. Castelli, B. Conti, D. E. Maccarrone, U. Conte, G. Puglisi, *Int. J. Pharm.* **1998**, *176*, 85–98. For recent reviews in antisense therapy and metabolite regulation, see: h) A. R. Yuen, B. I. Siki, *Front. Biosci.* **2000**, *5*, 588–593; i) S. M. Stepkowski, *Curr. Opin. Mol. Ther.* **2000**, *2*, 304–317; j) E. Uhlmann, *Curr. Opin. Drug Disc. Dev.* **2000**, *3*, 203–213; k) J. J. Schwartz, S. Zhang, *Curr. Opin. Mol. Ther.* **2000**, *2*, 162–167; l) A. A. Mountain, *Trends Biotechnol.* **2000**, *18*, 119–128.
- [2] a) D. T. Bong, T. D. Clark, J. R. Granja, M. R. Ghadiri, *Angew. Chem.* **2001**, *113*, 1016–1041; *Angew. Chem. Int. Ed.* **2001**, *40*, 988–1011; b) G. J. Kirkovits, C. D. Hall, *Adv. Supramol. Chem.* **2000**, *7*, 1–47.
- [3] J. R. Granja, M. R. Ghadiri, *J. Am. Chem. Soc.* **1994**, *116*, 10785–10786.
- [4] M. R. Ghadiri, J. R. Granja, L. K. Buehler, *Nature* **1994**, *369*, 301–304.
- [5]  $\beta$ -Amino acids have been successfully employed in the design of cyclic peptide-based transmembrane ion channels: T. D. Clark, L. K. Buehler, M. R. Ghadiri, *J. Am. Chem. Soc.* **1998**, *120*, 651–656.
- [6] K. Motesharei, M. R. Ghadiri, *J. Am. Chem. Soc.* **1997**, *119*, 11306–11312.
- [7] H. S. Kim, J. D. Hartgerink, M. R. Ghadiri, *J. Am. Chem. Soc.* **1998**, *120*, 4417–4424.
- [8] With respect to the surface normal, the tilt of the peptide tube axis was  $28.5 \pm 1^\circ$  and the lipid hydrocarbon chain tilt was  $26 \pm 2^\circ$ .
- [9] D. Schomburg, M. Salzmann, D. Stephan, *Enzyme Handbook*, Vol. 2, Springer, Berlin, **1990**.
- [10] This is an underestimation of the actual rate of transport since only a fraction of the total peptides are expected to self-assemble into transport-competent pores.
- [11] O. S. Smart, J. Breed, G. R. Smith, M. S. P. Sansom, *Biophys. J.* **1997**, *72*, 1109–1126.
- [12] Planar lipid bilayers from 1,2-diphytanoyl-*sn*-glycero-3-phosphocholine were prepared as described in M. Montal, P. Mueller, *Proc. Natl. Acad. Sci. USA* **1972**, *69*, 3561–3566. All electrolyte solutions employed were buffered with 3-(*N*-morpholino)propane sulfonic acid (MOPS; 5 mM; pH 7.5).
- [13] Conductance was observed to decrease at high NaCl concentrations (over 1 M). This is consistent with the presence of more than one ion inside the channel under those conditions, where the resulting repulsion diminishes the transport rate: W. D. Stein, *Channels, Carriers and Pumps: An Introduction to Membrane Transport*, Academic Press, San Diego, **1990**.
- [14] O. D. Bonner, *J. Chem. Eng. Data* **1981**, *26*, 147–148.
- [15] B. Hille, *Ionic Channels of Excitable Membranes*, Sinauer, Sunderland, **1991**.